Journal of Functional Foods 127 (2025) 106754

Contents lists available at ScienceDirect

Journal of Functional Foods

journal homepage: www.elsevier.com/locate/jff

Hydroxytyrosol, tyrosol and their phase II metabolites as inhibitors of endothelial cell inflammation induced by high glucose levels

Sonia Zodio [a,1], Gabriele Serreli [a,*,1], Anna Boronat [b,c], Rafael De la Torre [b,c,d], Maria Paola Melis [a], Monica Deiana [a]

[a] Department of Biomedical Sciences, University of Cagliari, Cittadella Universitaria SS 554, 09042 Monserrato, Italy
[b] Department of Medicine and Life Sciences, Universitat Pompeu Fabra, 08003 Barcelona, Spain
[c] Integrative Pharmacology and Systems Neurosciences Research Group, Hospital del Mar Research Institute, 08003 Barcelona, Spain
[d] Physiopathology of Obesity and Nutrition Networking Biomedical Research Centre (CIBEROBN), 28029 Madrid, Spain

ARTICLE INFO

Keywords:
Extra-virgin olive oil
Endothelial cells
HUVEC
Hyperglicemia
Metabolites
Phenolic compounds

ABSTRACT

The aim of this investigation was to evaluate the protective effect of the main extra-virgin olive oil (EVOO) phenolic compounds, HT and Tyr, and their phase II metabolites, against the inflammatory response in HUVEC monolayers under hyperglycemic conditions. The alteration of endothelial barrier in HUVEC, treated with high glucose (HG, 30 mM) alone or together with EVOO phenols (1 μM), was evaluated through FITC-Dextran cell permeability test and the determination of TJ proteins occludin, zonulin and JAM-A level, in relation to redox-sensitive MAPK modulation, NLRP3 protein level and cytokines release. Obtained data showed that HG-induced increase of permeability through the alteration of TJ proteins, following the activation of upstream pathways involved in the inflammatory process such as p38, ERK1/2 and NLRP3, was reverted by pre-treatment with EVOO phenols and their metabolites, strengthening the hypothesis that these dietary compounds may exert a significant role in the maintenance of endothelial barrier integrity.

1. Introduction

Endothelial cells (EC), which line the interior surface of blood vessels, play a critical role in maintaining vascular homeostasis (Rajendran et al., 2013). Hyperglycemic conditions, such as those found in diabetes mellitus, can induce endothelial dysfunction, primarily through the promotion of inflammatory pathways in EC (Funk, Yurdagul Jr., & Orr, 2012). Chronic inflammation induced by hyperglycemia in EC is a significant contributing factor to the development of cardiovascular diseases (CVD), which are prevalent complications of diabetes (Yamagishi, 2011). Some of these effects result from the production of advanced glycation end products (AGEs) and the interaction of these products with specific receptors (RAGE), which activate several downstream proinflammatory signaling cascades (C. Zhang, 2008). Tight junctions (TJ) modulation is among the final harmful events related to hyperglycemia at endothelial level. Indeed, high glucose (HG) levels compromise the integrity of TJ proteins, such as occludin, ZO-1 and claudins, which are essential for maintaining endothelial barrier function (Robles-Osorio & Sabath, 2023). Beyond the AGE-RAGE axis activation, hyperglycemia is also known to be able to increase the production of reactive oxygen species (ROS), which cause oxidative damage to cellular components and activate upstream signaling pathways (P. Gonzalez, Lozano, Ros, &

Abbreviations: AGE, advanced glycation end products; COX, cyclooxygenase; CTRL, control; CVD, cardiovascular disease; DAG, diacylglycerol; DAMPs, damage-associated molecular pattern molecules; EC, endothelial cells; ERK1/2, extracellular signal-regulated kinase 1/2; EVOO, extra-virgin olive oil; FITC-Dextran, fluorescein isothiocyanate-Dextran; HG, high glucose; HT, hydroxytyrosol; HT glu, 3′- hydroxytyrosol 3′-glucuronide; HT sulf, hydroxytyrosol 3-sulfate; HUVEC, human umbilical vein endothelial cells; IL-1β, interleukin 1β; IL-6, interleukin 6; JAM-A, junctional adhesion molecule A; LOX, lipoxygenases; LPS, lipopolysaccharide; MAPK, mitogen-activated protein kinase; MTT, 2,5-diphenyltetrazolium bromide; NF-κB, nuclear factor kappa-light-chain-enhancer of activated B cells; NLRP3, NOD-LRR- and pyrin domain-containing protein 3; NO, nitric oxide; NOS, nitric oxide synthase; PKC, protein kinase C; RAGE, receptor for advanced glycation end products; ROS, reactive oxygen species; TNF-α, tumor necrosis factor alpha; TJ, tight junctions; Tyr, tyrosol; Tyr glu, tyrosol glucuronide; Tyr sulf, tyrosol sulfate; XO, xanthine oxidases; ZO-1, zonula occludens 1.

* Corresponding author at: Department of Biomedical Sciences, University of Cagliari, Cittadella Universitaria SS 554, 09042 Monserrato, Italy.
E-mail address: gabriele.serreli@unica.it (G. Serreli).

[1] Sharing first coauthorship.

https://doi.org/10.1016/j.jff.2025.106754
Received 15 August 2024; Received in revised form 28 January 2025; Accepted 18 March 2025
Available online 26 March 2025

Solano, 2023). Indeed, through the alteration of cellular redox status, hyperglycemia is able to activate the redox-sensitive mitogen-activated protein kinases (MAPK), including ERK1/2 and p38, leading to the activation of the transcription factor NF-κB which in turn activates the expression of pro-inflammatory genes, increasing the production of inflammatory cytokines and adhesion molecules, and affecting the composition and location of TJ proteins (Cong & Kong, 2020; Yuan et al., 2019). In addition, hyperglycemia induces the release of damage-associated molecular patterns (DAMPs), which activate the NLRP3 inflammasome. This process results in the activation of caspase-1, which converts pro-inflammatory cytokines precursors, such as pro-IL-1β, into their active form (Schroder & Tschopp, 2010). Hence, the combined effects of NLRP3 inflammasome and NF-κB signaling activation result in the increased release of pro-inflammatory mediators, such as IL-1β, IL-6, and TNF-α, that amplify the inflammatory response by promoting the recruitment and activation of additional immune cells, further exacerbating endothelial dysfunction (C. Zhang, 2008).

Dietary phenolic compounds have garnered attention for their potential health benefits at the endothelial level, including anti-inflammatory properties (Pandey & Rizvi, 2009). Hydroxytyrosol (HT, 3′,4′-dihydroxyphenylethanol) and tyrosol (Tyr, 4′-hydroxyphenylethanol), two prominent phenols found in extra-virgin olive oil (EVOO), have shown to possess various biological activities that may contribute to endothelial homeostasis (Vijakumaran et al., 2023). These compounds are believed to exert protective effects by modulating intracellular signals involved in the onset of oxidative stress and inflammatory responses (Serreli & Deiana, 2020). The study of their bioavailability and metabolism is a crucial task to understand their biological significance for human health. HT and Tyr are usually absorbed in the small intestine, but they have low bioavailability due to extensive metabolism (Garcia-Villalba et al., 2010; Rubio et al., 2012). In fact, metabolic phase II reactions promote the conjugation of HT and Tyr with glucuronide and sulfate groups, resulting in high concentrations of glucuronidated and sulfated HT and Tyr forms in plasma and urine (Galmes, Reynes, Palou, Palou-March, & Palou, 2021) and in the nearly disappearance of their free forms which are deemed undetectable in biological matrices and in circulation (Serreli & Deiana, 2018). In addition, EC are able themselves to release different metabolites of HT and Tyr, thus contributing to reach physiologically relevant concentrations in the blood stream (Catalan et al., 2015). Our recent studies have demonstrated that glucuronidated and sulfated conjugates of HT and Tyr are biologically active at endothelial level, being able to preserve endothelial function by enhancing nitric oxide (NO) release (Serreli et al., 2021) and counteracting lipopolysaccharide (LPS)-induced inflammation and increase of permeability (Zodio et al., 2024).

In the present study we wanted to investigate the ability of HT and Tyr and their phase II metabolites to protect EC against hyperglycemia induced proinflammatory response. Their modulatory effect was evaluated in HUVEC cells subjected to HG conditions, focusing on the alteration of endothelial permeability related to ROS production and TJ proteins depletion. The activation of cellular pathways, as MAPK and NLRP3 inflammasome, and the production of IL-6 and IL-1β, which are linked to the EC proinflammatory response were also assessed.

2. Material and methods

2.1. Reagents and chemicals

Bovin Serum Albumin, 2,5-Diphenyltetrazolium Bromide (MTT), 2,7- dicloroflouresceindiacetate, fluorescein isothiocyanate-dextran (wt 4000), dimetyl-sulfoxide (DMSO), Bradford reagent, CellLytic-M, D-glucose, hydroxytyrosol, tyrosol, NaCl, Tween 80 and all solvents of analytical grade were purchased from Sigma Aldrich (Milano, Italy). Tyrosol glucuronide (phenylethanol-4′-glucuronide), tyrosol sulfate sodium salt (phenylethanol-4′-sulfate), 3′- hydroxytyrosol 3′-glucuronide (4′-hydroxyphenylethanol-3′-glucuronide) and hydroxytyrosol 3-sulfate sodium salt (4′-hydroxyphenylethanol-3′-sulfate) were obtained from LGC standards (Sesto San Giovanni, Italy). Phosphatase and Protease Inhibitor Cocktail, nitrocellulose membranes, gels and all material for electrophoresis and immunoblotting, SYBR Green qPCR Master Mixes, High Capacity cDNA Reverse Transcription kit were purchased from ThermoFisher Scientific (Massachusetts, United States). RNeasy Mini Kit were purchased from Qiagen (Germany).

2.2. Materials for HUVEC cells

The HUVEC cell line were obtained from Lonza (Basel, Switzerland). The medium EBM-2 with phenol red, the BulletKit™ – basal medium and SingleQuots™ and ReagentPack Subculture Reagents with Trypsin/EDTA, TNS (Trypsin Neutralizer solution) and HEPES (4-(2-hydroxyethyl)-1 piperazineethanesulfonic acid) solutions were obtained from Lonza (Basel, Switzerland).

2.2.1. Maintenance of HUVEC cell culture

HUVEC cells were maintained in T75 flasks until they reached confluence in EBM-2 supplemented with 2 % FBS, 0.2 % heparin, 0.2 % hydrocortisone, 0.2 % hFGFb (Human Fibroblast Growth Factor basic), 0.2 % hVEGF (Human Vascular Endothelial Growth Factor), 0.2 % long R3-IGF-1 (analog of Human Insulin-Like Growth Factor-1), 0.2 % ascorbic acid, 0.2 % hEGF (Human Epidermal Growth Factor) and 0.2 % of GA 1000 (gentamycin sulfate) at 37 °C in a 5 % CO_2 humidified atmosphere. The subcultures were prepared by removing the cells with ReagentPack Subculture Reagents washing with HEPES, adding trypsin and neutralizing with TNS, and then seeded into 96-well, 6-well and transwell plates at a concentration of 5×10^4 /mL or 7.5×10^4 /mL for different experiments. Cells were cultured for 5–7 days, replacing the medium twice a week.

2.3. MTT assay

The MTT (3-(4,5-dimethylthiazol-2-yl)-2,5-diphenyltetrazolium bromide) assay was performed as reported by Serreli et al. (Serreli et al., 2021). Briefly, cells were exposed to all the compounds tested in this study (1 μM, 2,8–6,6 μL of 0.1 mg/mL solution dissolved in 2 mL serum free medium), or an equivalent volume of vehicle (MeOH, 5 μL dissolved in 2 mL serum free medium, 0.25 %) for the controls (0 μM) and incubated for 24 h with HG (final concentration 30 mM). After the treatments, the medium was replaced by 100 μL of MTT solution (0.5 mg/mL in supplemented growth media) and left for 4 h at 37 °C. The medium was removed, 100 μL of DMSO were added in each well and the absorbance was read at 570 nm by using a micro plate reader (Infinite 200, Tecan, Salzburg, Austria). After subtracting the blank values, data were converted to % of cells viability as follows: % cell viability = Abs sample/Abs control × 100.

2.4. Determination of monolayer permeability

Changes in HUVEC monolayer permeability exposed to HG were assessed by the FITC-Dextran Permeability assay. HUVEC (1×10^5 cells/mL) were seeded on transwell filters (0.4-um pore size, Costar, New York, USA) in 12-well plates and grown until they reached confluence. Then, cells were treated with HG (final concentration 30 mM) for 2 h, 4 h, 6 h, 18 h and 24 h, or were pre-treated with Tyr, HT and their sulfated and glucuronidated metabolites (1 μM) for 24 h before adding the HG (30 mM final concentration) solution for 3 h. After treatment, the medium was replaced with Fluorescein isothiocyanate (FITC)-Dextran solution in the upper chamber at a final concentration of 1 mg/mL. After 1 h incubation at 37 °C, paracellular flux was assessed by taking 100 μL aliquots from both chambers to measure real-time changes of permeability across endothelial cell monolayers Fluorescence was measured at emission wavelengths of 485 and 530 nm (X. Zhang et al., 2013). The concentration of basal permeable FITC-Dextran was calculated

compared to control samples.

2.5. Determination of intracellular ROS production

ROS production in HUVEC was determined using the fluorescent probe 2′,7′- DCFH-DA, according to Deiana and others (Deiana et al., 2019) with minor modifications. HUVEC cells were seeded in 96-well culture plates and once confluent were incubated for 24 h with Tyr, HT and their sulfated and glucuronidated metabolites (1 μM in complete medium) or an equivalent volume of MeOH for the controls. The medium was then removed and 100 μL of 2′,7′- DCFH-DA solution in PBS (10 μM) were added in each well and left for 20–30 min in the dark. Subsequently, the medium was replaced by 100 μL of HG solution (final concentration 30 mM in PBS) and the fluorescence of 2′,7'-DCFH-DA was determined using a micro plate reader by recording the emission signal at 525 nm after excitation signal at 488 nm every five minutes in a time range of 2 h.

2.6. Western blot analyses

To investigate the TJ and NLRP3 inflammasome proteins, and phosphorylated MAPK by Western blot analyses, the samples were prepared as previously described (Zodio et al., 2024). HUVEC cells seeded in 6-well plates (5×10^4 or 7.5×10^4 cells/mL in 2 mL of growth media), were treated with HG (final concentration 30 mM) for different incubation times based on the protein to be analysed, or were pre-treated with Tyr, HT and their sulfated and glucuronidated metabolites (1 μM) for 24 h before adding the HG (30 mM) solution for 3 h. After incubation the medium was removed and 180 μL lysis buffer (supplemented with phosphatase and protease inhibitor) was added. Protein concentration was determined through Bradford assay (Bradford, 1976). Denatured proteins (20–40 μg) were separated using 4–12 %, 10 % and 4–20 % polyacrylamide gel, then transferred into nitrocellulose membranes blocked with 25 mL of a TBS and 4 % milk solution for 40 min. After washing with TBS solution, membranes where incubated overnight, at 4 °C, with primary polyclonal antibodies, anti-ERK1/2, anti-phospho ERK1/2, anti-phospho p38, anti-p38 (Cell Signaling Technology, Danvers, Massachussets, USA), anti-β actin, anti-GADPH, anti-JAM-A, anti-ZO-1, anti-Occludin (Abcam, Cambridge, UK), anti-NLRP3 (Sigma Aldrich, Milan, Italy), and then washed two times with TTBS (TBS with Tween 20 0.5 %) before adding the secondary rabbit and/or mouse antibody IgG peroxidase-conjugated (Sigma Aldrich, Milan, Italy). Both primary and secondary antibody were prepared adding an aliquot of the original solution in 10 mL of TTBS solution with 1 % of milk (dilution 1:1000 *v*/v). Membranes were washed twice with TTBS and one time with TBS, exposed to Clarity™ Western-ECL reagents (4–5 min) and observed through ChemiDoc™ MT System. The bands were displayed by using the ChemiDoc™ XRS + System (Bio-Rad Laboratories, Inc., Hercules, CA, USA). The molecular weights of the protein bands were deduced from a comparison with pre-stained molecular weight markers that were run in parallel with the cell samples (range 14–180 kDa, GenScript, Piscataway, NJ, USA). Protein bands were dosed using Quantity One software (BioRad Laboratories).

2.7. Gene expression by qRT-PCR

Confluent HUVEC cells in 6-well plates (5×10^4 cells/mL in 2 mL of growth media), were pre-treated with Tyr, HT and their sulfated and glucuronidated metabolites (1 μM) for 24 h before adding HG (final concentration 30 mM) for 2 h and 6 h. The medium was then removed and 200 μL of free RNAse was added and supernatant collected and stored at −20 °C. Total RNA was extracted from the HUVEC with RNeasy Mini Kit (Qiagen, Germany). The High-Capacity cDNA Reverse Transcription kit (Thermo Fischer Scientific) was used to reverse transcribe RNA to cDNA through the thermocycler (Mastercycler gradient, Eppendorf) according to the manufacturer's instructions.

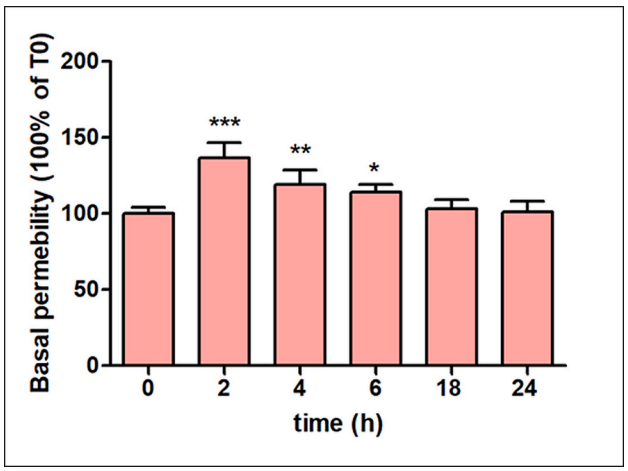

Fig. 1. FITC-Dextran basal permeability measured in untreated HUVEC cells (T0) or treated with HG (30 mM) at 2 h, 4 h, 6 h, 18 h and 24 h incubation times. Data are reported as percentage compared to T0 for each time. * = $p < 0.05$ vs time 0; ** = $p < 0.01$ vs time 0; *** = $p < 0.001$ vs time 0 ($n = 6$).

The conditions of thermal cycling were as follow: step 1: 25 °C for 10 min; step 2: 37 °C for 120 min; step 3: 85 °C for 5 min and final step at 4 °C. The relative expression level of genes was analysed using SYBR Green qPCR Master Mixes (Thermo Fisher Scientific) and the sequences of PCR primers used were as follows: IL-1β (Forward and Reverse), IL-6 (Forward and Reverse), and β-actin (Forward and Reverse) (SigmaAldrich, Milan, Italy). β-actin was used as an internal control using 2-ΔΔCT. Gene expression was measured by a real-time polymerase chain reaction with a QuantStudio™ 12 K Flex RealTime PCR System (Applied Biosystems, Foster City, CA, USA). Results were obtained with the Expression Suite Software v1.0.3 (Applied Biosystems, Foster City, CA, USA).

2.8. Statistical analysis

The statistical analysis was performed using the average ± standard deviations for each of the groups in all the experiments (each experiment was performed at least 3 times); significative differences were found through the software GraphPad Prism 5 (GraphPad software, San Diego, CA, USA), using the analysis of variance "one-way ANOVA" and posthoc Bonferroni's test.

3. Results

3.1. Cell viability

Cell viability was assessed in HUVEC monolayers to exclude any possible cytotoxic effects of the tested compounds (1 μM) co-incubated with HG (30 mM) using the MTT, 3-(4,5-dimethylthiazol-2-yl)-2,5-diphenyltetrazolium bromide, test. The treatment conditions did not affect significantly HUVEC cell viability ($p > 0.05$) after 24 h of incubation, resulting in an absence of significant change in cell viability (**Figure S1**).

3.2. Alteration of HUVEC monolayer permeability

The capacity of HG to induce alteration of endothelial permeability was evaluated in vitro in HUVEC cell monolayers by measuring FITC–Dextran flux. Cells were treated with HG (30 mM) and incubated for 2 h, 4 h, 6 h, 18 h and 24 h, at the end of which the basal permeability of FITC-Dextran was measured spectrophotometrically. In addition, the ability of the phenolic compounds, tested at non toxic concentrations, to limit the alteration of endothelial permeability induced by HG after 2 h

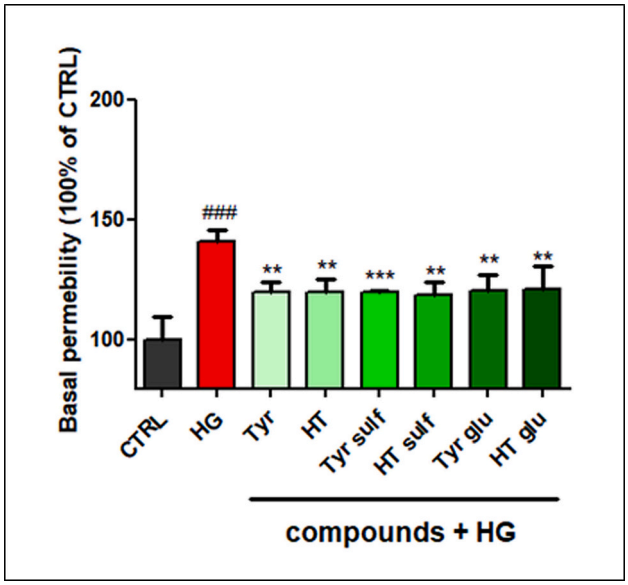

Fig. 2. FITC-Dextran basal permeability measured in HUVEC cells pretreated with Tyr, HT, Tyr sulf, HT sulf, Tyr glu, HT glu (1 μM) or with an equivalent volume of MeOH (CTRL), and treated with HG (30 mM) for 2 h. Data are reported as percentage compared to CTRL for each sample. ** = p < 0.01 vs HG; *** = $p < 0.001$ vs HG; ### = p < 0.001 vs CTRL (n = 6).

incubation was also detected. The changes in HUVEC cell monolayers permeability induced by HG treatment are shown in Fig. 1. A significant increase in permeability, about 35–40 % compared to the untreated cells (time 0), was observed at 2 h of treatment. The monolayer permeability decreased subsequently over time, returning to baseline levels by 18 h of incubation. Based on this observation, we chose to conduct permeability studies at 2 h post-HG treatment. Fig. 2 shows the change in endothelial permeability induced by HG treatment in HUVEC cells pretreated with the tested phenolic compounds and their metabolites for 2 h. Phenolic compounds counteracted FITC-Dextran basal permeability increases (about 40 % respect to the CTRL), exerting a protective action on the endothelial monolayer, which was almost equally for all tested compounds (HT sulf vs HG $p < 0.001$, the other compounds vs HG $p < 0.01$).

3.3. ROS production

In order to evaluate the effect of HG-treatment and EVOO phenolic metabolites on cellular redox status, we measured ROS generation in HUVEC cells, treated with HG (30 mM) and pretreated with HT, Tyr and their metabolites (1 μM) using 2′,7′-DCFH-DA assay. Treatment with HG resulted in a significant increase of ROS production starting from 30 min of incubation (about 40 %) and continuing to increase in a time-dependent increase (50 % at 1 h of incubation and 60 % at 2 h of incubation) in comparison with the CTRL (Fig. 3). Pretreatment with the phenolic compounds and their sulfated and glucuronidated metabolites counteracted HG-induced alteration of cellular redox status, inhibiting ROS production. Notably, all compounds prevented ROS formation in a similar way ($p < 0.05$ Tyr vs HG, $p < 0.001$ the other compounds vs HG).

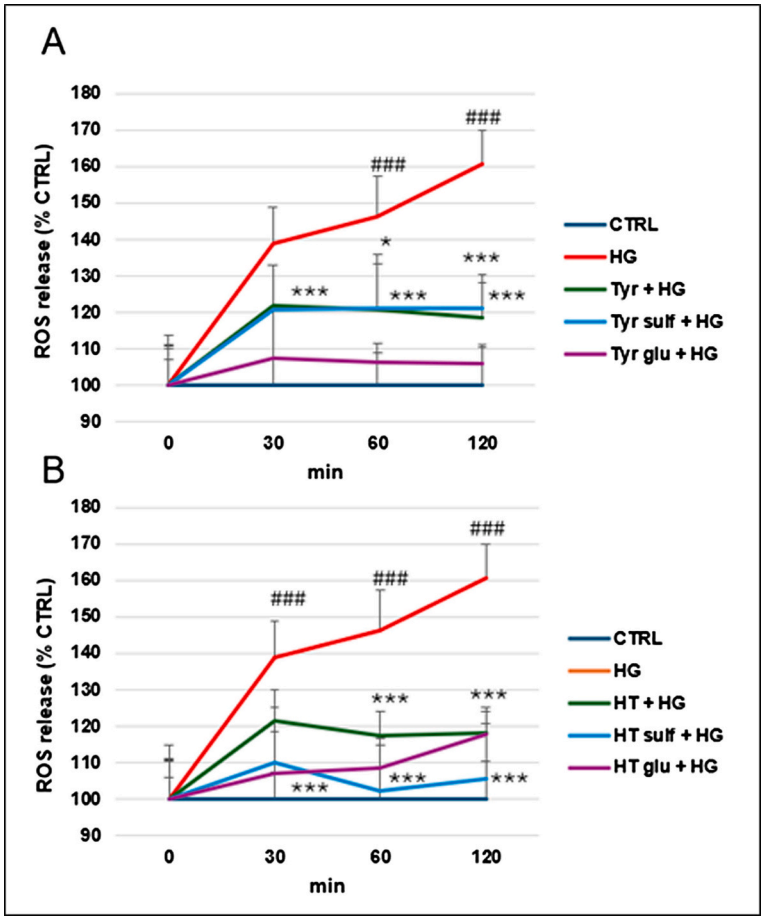

Fig. 3. ROS levels, visualized as H2-DCF-DA fluorescence and expressed as % of the control samples (CTRL, non-oxidized nor pretreated samples), in HUVEC after 1 h incubation with Tyr, Tyr sulf, Tyr glu (A), HT, HT sulf, HT glu (B) (1 μM) in co-incubation with HG (30 mM). * = p < 0.05 vs HG; *** = p < 0.001 vs HG; ### = p < 0.001 vs CTRL ($n = 18$).

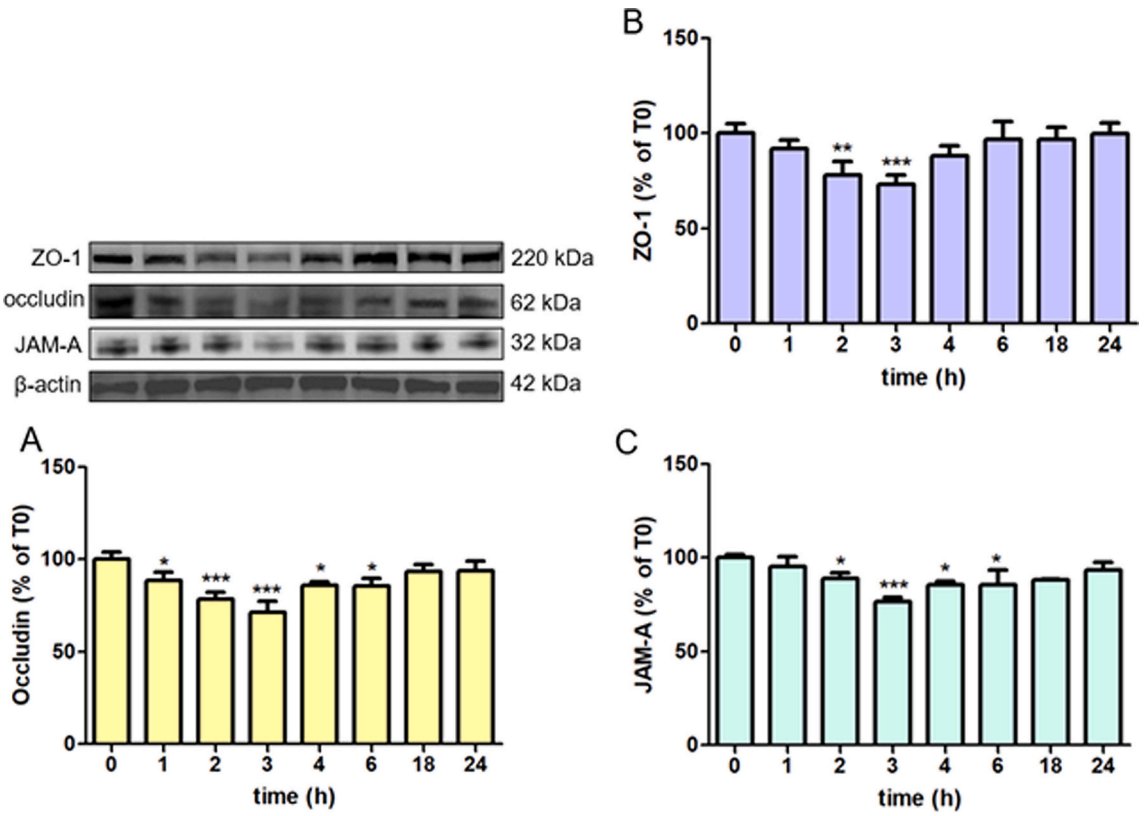

Fig. 4. Occludin **(A)** ZO-1 **(B),** and JAM-A **(C)** /β-actin ratio measured in HUVEC cells before treatment (time 0) or treated with HG (30 mM) at different incubation time (1, 2, 3, 4, 6, 18 and 24 h). Data are reported as percentage compared to time 0 for each time. * = $p < 0.05$ vs time 0; ** = $p < 0.01$ vs time 0; *** = $p < 0.001$ vs time 0 ($n = 3$). Representative WB images of the experiment are shown.

3.4. Modulation of TJ proteins

The HG-induced alteration in HUVEC cell monolayers, focusing on the modulation of TJ proteins occludin, ZO-1 and JAM-A with time, was investigated through Western blotting. Cells were treated with HG (30 mM) for 1, 2, 3, 4, 6, 18 and 24 h to observe any effects on TJ protein level. As shown in Fig. 4, HG induced a significant decrease of occludin (Fig. 4A), ZO-1 (Fig. 4B) and JAM-A (Fig. 4C) levels in HUVEC, with a percentage of about 25–30 % reduction with respect to the CTRL (100 %) at 3 h, confirming the role of HG in endothelial barrier alteration. From 6 h to 24 h the disrupting effect of HG on all three TJ proteins was not significant, as we detected levels similar to untreated cells (time 0). Fig. 5 shows the protective effect of the phenolic compounds against HG-induced decrease in occludin (Fig. 5A), ZO-1 (Fig. 5B) and JAM-A (Fig. 5C) levels, exerted in HUVEC in co-incubation with HG for 3 h. HG led to a decrease of about 25–30 % of TJ proteins level compared to CTRL (100 %). Pretreatment with Tyr, HT and their sulfated and glucuronidated metabolites significantly limited the HG-induced decrease of all TJ proteins, with the same effectiveness.

3.5. Modulation of MAPK and NLRP3

Among the signaling pathways involved in the modulation of HUVEC monolayer permeability activated by HG, we focused on MAPK p38 and ERK1/2 and NLRP3 inflammasome. Firstly, cells were treated with HG (30 mM) for 1, 2, 3, 4 and 6 h to observe any significant change in MAPK phosphorylation and NLRP3 protein level. Fig. 6 shows the NLRP3 expression (Fig. 6A) and the phosphorylation rate of p38 (Fig. 6B) and ERK1/2 (Fig. 6C) detected in HUVEC cells treated with HG. After 2–3 h of incubation, HG induced a significant phosphorylation of both proteins with respect to the untreated cells (time 0), with an increase that was about 30 % for p-p38 and about 35 % for p-ERK1/2. At 6 h the level of both MAPK was similar to that of time 0. In addition, HG treatment determined a significant increase of NLRP3 protein levels of about 25–30 % compared to time 0 (100 %), and the higher value occurred at 3 h of incubation with HG. Starting from the fourth hour of incubation, the NLRP3 level showed no significant differences compared to time 0 values.

Pretreatment with the phenolic compounds significantly limited the phosphorylation of p38 and ERK1/2 with respect to the cells treated with only HG (**Fig. 7B** and **C**). The efficacy of the tested compounds was comparable, although with some exceptions. HT and Tyr glu, for instance, did not significantly modulate p38 phosphorylation. Pretreatment with the phenolic compounds also reduced the levels of NLRP3 protein to the extent of 22–30 % compared to HG group (Fig. 7A). This protective effect was observed for all the tested compounds, with differences in effectiveness ($p < 0.001$ Tyr sulf, HT sulf and Tyr glu vs HG; $p < 0.01$ HT and Tyr vs HG; $p < 0,05$ HT glu vs HG).

3.6. Interleukin expression

To further evaluate the role of HT, Tyr and their metabolites on the modulation of inflammatory response induced by HG, involving the activation of NLRP3, MAPK and NF-κB, we determined changes in the gene expression of IL-1β and IL-6 (products of NLRP3 and NF-κB pathways respectively) by RT-PCR analysis. HUVEC cells were pretreated with HT, Tyr and their glucuronidated and sulfated metabolites (1 μM) for 24 h and then treated with HG (30 mM), at 2 h and 6 h. Treatment with HG triggered a significant increase of the expression of the two cytokines at both incubation times (from about 30 % at 2 h to 70 % at 6 h of incubation), in comparison with the untreated cells (Fig. 8). Pretreatment with the phenolic compounds and their metabolites led to a significant containment of IL-1β and IL-6 production, exerting a protective action. The greatest effect was observed at 6 h. Glucuronidated

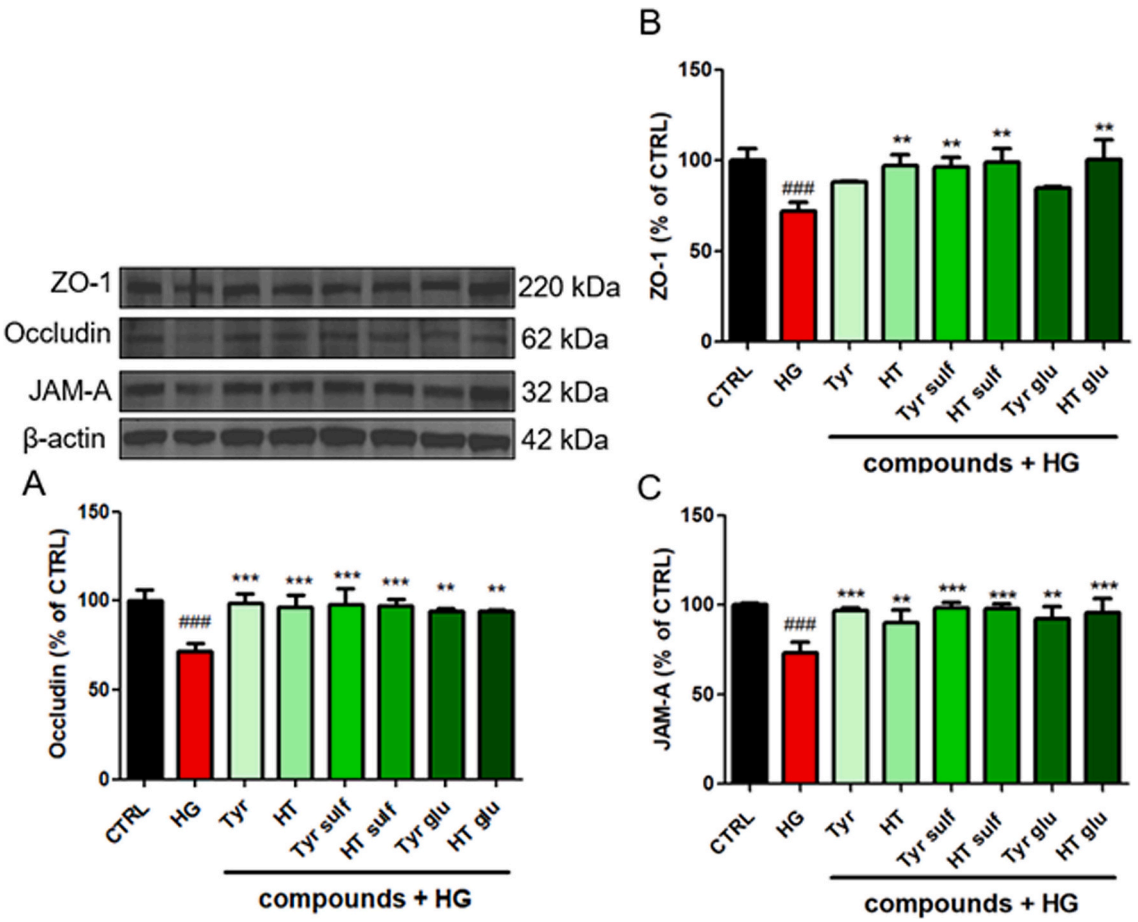

Fig. 5. Occludin **(A)** ZO-1 **(B),** and JAM-A **(C)** /β-actin ratio measured in cells pretreated with Tyr, HT, Tyr sulf, HT sulf, Tyr glu, HT glu (1 μM) and treated with HG (30 mM) for 3 h of incubation. Data are reported as percentage compared to CTRL for each sample. ** = $p < 0.01$ vs HG; *** = $p < 0.001$ vs HG; ### = $p < 0.001$ vs CTRL ($n = 3$). Representative WB images of the experiment are shown.

metabolites resulted to be more active after 2 h than the other compounds. However, at 6 h, all compounds limited the expression of both cytokines, in a similar manner, with no significant differences.

4. Discussion

Hyperglycemia is among the main risk factors involved in the onset and progression of CVD (Rezabakhsh et al., 2017). This effect is likely due to the accelerated formation of ROS and AGE, leading to endothelial dysfunction (Popov, 2010). Conversely, endothelial barrier function may be enhanced with the intake of compounds with antioxidant and anti-inflammatory properties like dietary phenolic compounds (Caminiti et al., 2024). However, they are poorly absorbed and/or extensively metabolized within enterocytes, liver and EC by phase I/II enzymatic reactions (Zeka, Ruparelia, Arroo, Budriesi, & Micucci, 2017). It is established that less than 5 % of the total phenolic intake is absorbed and reaches the plasma unchanged (Cao, Chen, Jassbi, & Xiao, 2015), therefore the parent compounds reach very low systemic levels that are unlikely to supply efficient cellular concentrations to justify the overall efficacy (Chiou et al., 2014). Thus, in the last years, an increasing interest has been paid to the metabolism of dietary phenolic compounds and the potential bioactivity of their metabolites with respect to the parent compounds (Serreli & Deiana, 2019). HT and Tyr are the main bioactive phenolic compounds present in EVOO that usually undergo biotransformation to produce mainly glucuronidated and sulfated metabolites, which have already been demonstrated to retain most of the beneficial effects of their parent compounds (Serreli, Le Sayec, Diotallevi, et al., 2021; Serreli, Melis, Corona, & Deiana, 2019; Zodio et al., 2024).

Herein, we aimed at evaluating for the first time the protective effect of HT, Tyr and their sulfated and glucuronidated metabolites against the inflammatory response at endothelial level induced by HG conditions. Their modulatory action was investigated in relation to oxidative stress, TJ proteins alteration and activation of upstream cellular pathways. The compounds of interest were tested in HUVEC monolayers at the concentration of 1 μM, considered to be biologically relevant in humans after ingestion of foods containing these phenols (Jenner, Rafter, & Halliwell, 2005; Manach, Scalbert, Morand, Remesy, & Jimenez, 2004; Pastor et al., 2016; Serreli et al., 2019) and in particular of EVOO and VOO, with plasma and urine values even higher (Galmes et al., 2021; Rubió et al., 2014). HUVEC were treated with a glucose concentration of 30 mM, reported to be the ideal concentration to analyse, in vitro, the HG-induced dysfunction of the vascular endothelium (Chang et al., 2014; Leng et al., 2019; Li et al., 2017). Chao and colleagues (Chao, Lee, Juo, & Yang, 2016) showed that HG 30 mM mediated the increase of vascular permeability in HUVEC without cause significant cytotoxicity. Even in our experimental conditions the incubation of HUVEC with HG 30 mM for 24 h, alone or in presence of the phenolic compounds, did not alter cell viability. HG exposure determined a significant and time-dependent increase of HUVEC monolayers permeability at 2–6 h of incubation confirming what previously reported by Chao et al. (Chao et al., 2016). Tyr, HT and their metabolites exerted their protective action after 2 h of treatment, with an equal trend for all the compounds tested. HG-induced increase of monolayer permeability was due, at least in part, to an alteration of TJ proteins, as demonstrated by the decrease, over time, of occludin, JAM-A and ZO-1 levels. Conversely, TJ proteins

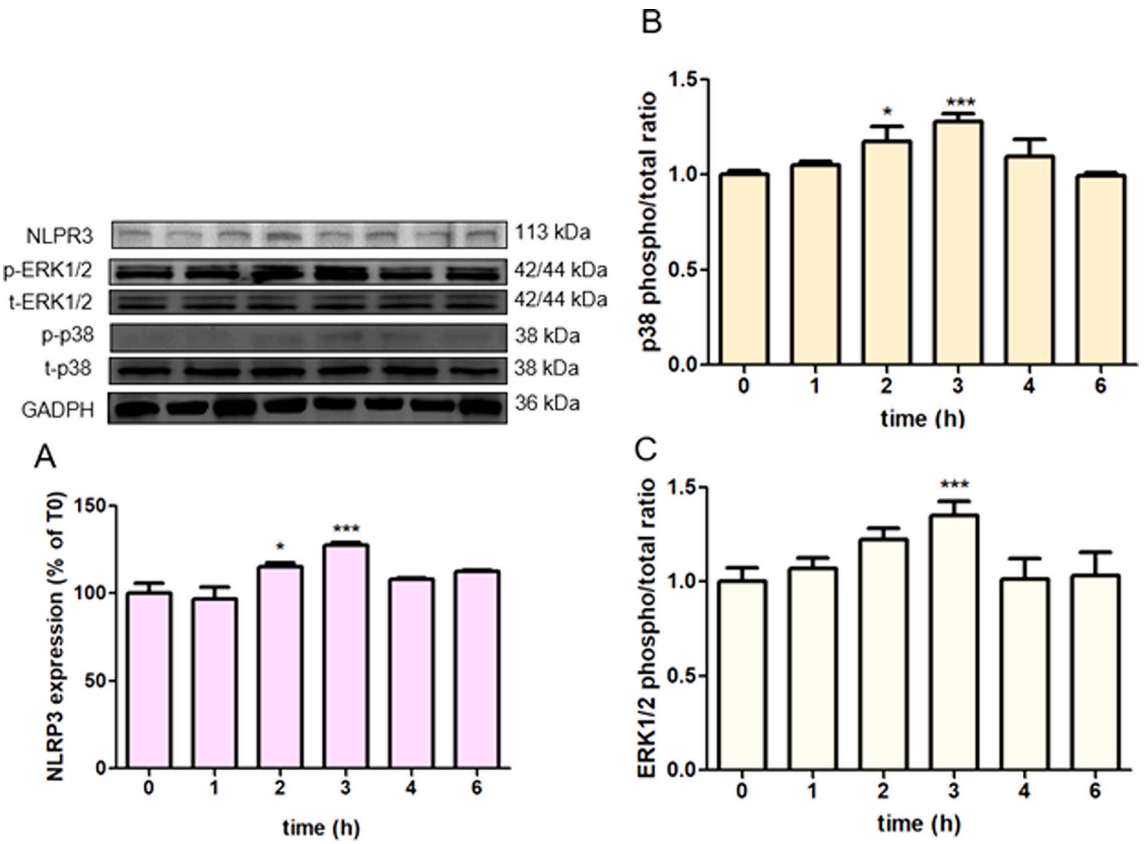

Fig. 6. NLRP3/β-actin **(A)**, p-p38/t-p38 **(B)** and p-ERK1/2/t-ERK1/2 **(C)** ratios measured in HUVEC cells not treated (time 0) or treated with HG (30 mM) at different incubation time (1, 2, 3, 4 and 6 h) ($n = 3$). * = $p < 0.05$ vs time 0; *** = $p < 0.001$ vs time 0. Representative WB images of the experiment are shown.

level was preserved by pretreatment with all the tested phenolic compounds, with some differences in effectiveness between some of the compounds, as evidenced by a lack of significant activity of Tyr and Tyr sulf on protecting ZO-1 against HG-induced depletion.

The increase in endothelial permeability induced by hyperglycemia has also been correlated to oxidative stress. This pathological condition is well-known to enhance intracellular ROS generation, further contributing to the dysfunction of EC (Lin et al., 2020; Qian et al., 2010). Hyperglycemia is known to activate a metabolic route that involves diacylglycerol (DAG) protein kinase C (PKC) and NADPH-oxidase, culminating in ROS release. Additionally, hyperglycemia induces ROS production in diabetic patients through mitochondrial respiratory chain enzymes, xanthine oxidases (XO), lipoxygenases (LOX), cyclo-oxygenases (COX), NO synthases (NOS), and peroxidases (Volpe, Villar-Delfino, Dos Anjos, & Nogueira-Machado, 2018). In our experimental conditions, HG treatment led to a significant and time dependent increase of ROS production in HUVEC, while pretreatment with Tyr, HT and their metabolites counteracted HG-induced alteration of cellular redox status. Notably, all compounds prevented ROS formation in a similar way, with some slight differences regarding Tyr sulf activity. Tyr and HT give a further demonstration of their well-known ability to contain oxidative stress, acting as direct scavengers of reactive species or inhibiting their generation in the cellular environment (Karkovic Markovic, Toric, Barbaric, & Jakobusic Brala, 2019); such ability is retained in their sulfated and glucuronidated metabolites, although several previous research showed how HT and Tyr lose much of their antioxidant capacity once conjugated (Serreli & Deiana, 2018). In addition, the inhibitory action on ROS led by EVOO phenols could derive from a direct action on some of HG-activated enzymes such as NADPH oxidase, as previously observed by Sun et al. (Sun et al., 2019).

Alterations of cellular redox status activate intracellular signaling pathways, as redox-sensitive MAPK (Plotnikov, Zehorai, Procaccia, & Seger, 2011). In our HUVEC monolayers HG-induced alteration of cellular redox status led to the activation of p38 and ERK1/2, confirming the involvement of MAPK pathways in HG-induced endothelial monolayer alteration. Indeed, the activation of p38 and ERK pathways by HG in HUVEC cells has also previously reported (M. H. Kim, Kim, & Kim, 2018; S. W. Kim, Kim, & Kim, 2011) as upstream event in the upregulation of Intercellular Adhesion Molecule 1 (ICAM1). In fact, phosphorylated MAPK may in turn promote the transcription of pro-inflammatory genes, involving NF-κB activation, which induces adhesion molecules, such as VCAM-1 and ICAM-1, increasing the migration and the adhesion of monocytic cells to EC, a key event of the proinflammatory response (Gloire, Legrand-Poels, & Piette, 2006). Moreover, the activation of the MAPK pathway is involved in the redistribution and destruction of TJ proteins (Cong & Kong, 2020) and may therefore be involved in the increased endothelial permeability observed in this study. Almost all compounds, with the exception of HT and Tyr glu, demonstrated significant efficacy in preventing p38 activation, while HT glu was the only one not to be active in counteracting ERK1/2 phosphorylation. HG has been also shown to activate NLRP3 inflammasome in several cell types (Wan et al., 2019), including endothelial cells (Gora, Ciechanowska, & Ladyzynski, 2021). In our experimental model, HG treatment induced an increase of NLRP3 protein level with time, which was inhibited by exposure to all tested phenolic compounds. We can assume that there is an antioxidant effect underlying the inhibitory effects on NLRP3 activation, since the HG-induced ROS release is known to play an essential role in the inflammasome activation, and the inhibition of ROS with specific scavengers is thought to suppress inflammasome activation in response to a range of NLRP3 activators (Gora et al., 2021). As a consequence of the activation by HG of all the signals we have previously described, the final production of proinflammatory cytokines such as IL-6 and IL-1β occurs, leading to direct effects on nearby cells and perpetuating the inflammatory response (Liu et al.,

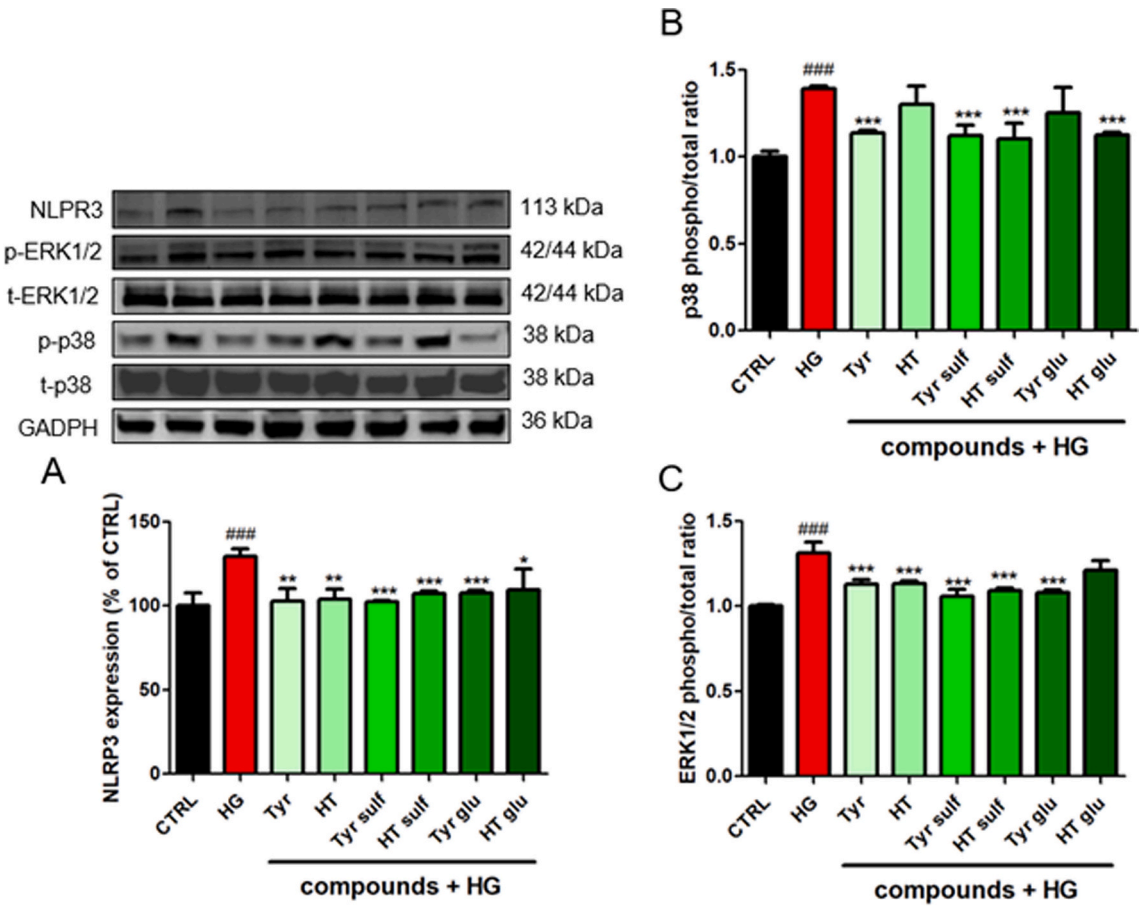

Fig. 7. NLRP3/β-actin **(A)**, p-p38/t-p38 **(B)** and p-ERK1/2/t-ERK1/2 **(C)** ratios measured in HUVEC cells pretreated with Tyr, HT, Tyr sulf, HT sulf, Tyr glu, HT glu (1 μM) or with an equivalent volume of MeOH (CTRL), and treated with HG (30 mM) for 3 h. * = $p < 0.05$ vs HG; ** = $p < 0.01$ vs HG; *** = $p < 0.001$ vs HG; ### = $p < 0.001$ vs CTRL ($n = 3$). Representative WB images of the experiment are shown.

2021). As expected, HT, Tyr and their metabolites were also effective in inhibiting the gene expression of the proinflammatory cytokines IL-1β, produced after NLRP3 activation (Pavillard, Marin-Aguilar, Bullon, & Cordero, 2018) and IL-6, produced after NF-κB translocation into the nucleus (Brasier, 2010), which were overexpressed in HG-treated HUVEC. The greatest efficacy was observed after 6 h of treatment, where all the tested compounds even lowered the levels of interleukins compared to the control levels. This outcome demonstrates that, although some compounds failed to modulate a specific signaling pathway, the overall effect carried out in HUVEC resulted in an inhibition of the proinflammatory response on the endothelial monolayer, as evidenced by and the reduction of IL-6 and IL-1β gene expression.

Once again sulfated and glucuronidated metabolites have shown the comparable efficacy of parent compounds in exerting a biological action. However, it should be considered that these conjugates could be easily deconjugated within the cells, potentially leading to the formation of new metabolites produced by ECs. Consequently, the overall beneficial action observed in our study can be attributable to a complex and dynamic pool of metabolites that are continuously changing in the endothelial environment (Boronat et al., 2021). Therefore, a potential weakness is the in vitro nature of the study, which may not fully capture the complexity of in vivo systems, particularly concerning the dynamic metabolism and potential deconjugation processes of these compounds within the human body. Future studies incorporating clinical trials would be invaluable to validate these findings.

In conclusion, this study underscores the significant protective effects of HT, Tyr, and their phase II metabolites on endothelial cells exposed to HG conditions. Hyperglycemia-induced endothelial dysfunction, characterised by increased permeability, oxidative stress, and inflammation, is a critical factor in the progression of CVD. Our results demonstrate that these dietary compounds present in EVOO effectively counteract these adverse effects by preserving TJ protein integrity and inhibiting the increase of permeability by suppressing the activation of the MAPK pathway and NLRP3 inflammasome, also reducing the expression of pro-inflammatory cytokines IL-1β and IL-6. More complex mechanisms however, as a direct action of these phenolic compounds on the AGE/RAGE axis, which is upstream of MAPK and NLRP3 signaling pathways, cannot be excluded (I. Gonzalez, Morales, & Rojas, 2020; Hu et al., 2023; Kong et al., 2017).

Overall, despite the limited bioavailability of dietary HT and Tyr, their metabolites retain significant bioactivity. This suggests their potential as therapeutic agents in mitigating endothelial inflammation and dysfunction associated with hyperglycemia. Our findings provide a deeper understanding of the molecular mechanisms by which HT, Tyr, and their metabolites exert their protective effects, paving the way for future research on their clinical applications in preventing CVD in diabetic patients.

Ethic Statement

This article does not contain any clinical trials or studies involving animals performed by any of the authors.

CRediT authorship contribution statement

Sonia Zodio: Methodology, Investigation, Data curation,

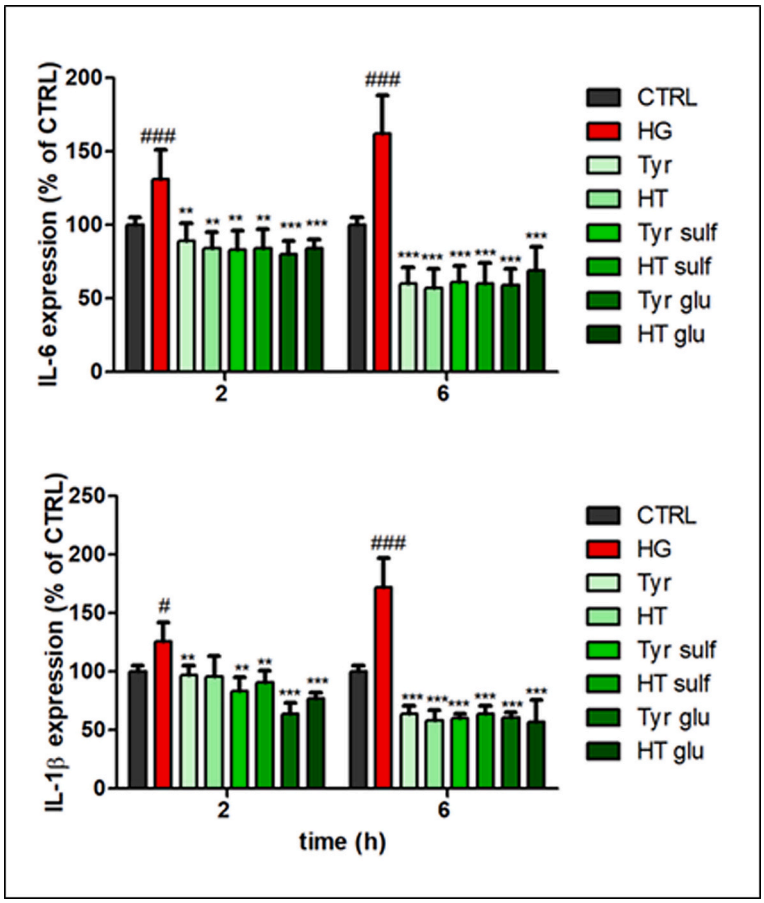

Fig. 8. IL-6 and IL-1β expression measured by RT-PCR analyses in HUVEC incubated with Tyr, HT, Tyr sulf, HT sulf, Tyr glu, HT glu (1 μM) or with an equivalent volume of MeOH (CTRL), and treated with HG (30 mM) for 2 h and 6 h. ** = $p < 0.01$ vs HG; *** = $p < 0.001$ vs HG; # = $p < 0.05$ vs CTRL; ### = $p < 0.001$ vs CTRL; ($n = 6$).

Conceptualization. **Gabriele Serreli:** Writing – review & editing, Writing – original draft, Visualization, Methodology, Investigation, Formal analysis, Data curation, Conceptualization. **Anna Boronat:** Writing – review & editing, Investigation, Formal analysis, Data curation. **Rafael De la Torre:** Writing – review & editing, Visualization, Supervision, Funding acquisition. **Maria Paola Melis:** Writing – review & editing, Supervision, Investigation, Formal analysis, Data curation. **Monica Deiana:** Writing – review & editing, Writing – original draft, Visualization, Supervision, Project administration, Funding acquisition, Data curation, Conceptualization.

Funding

The author(s) declare financial support was received for the research, authorship, and/or publication of this article. This research was funded by the University of Cagliari (FIR – supplementary research fund year 2022).

Declaration of competing interest

The authors declare that they have no known competing financial interests or personal relationships that could have appeared to influence the work reported in this paper.

Appendix A. Supplementary data

Supplementary data to this article can be found online at https://doi.org/10.1016/j.jff.2025.106754.

Data availability

Data will be made available on request.

References

Boronat, A., Rodriguez-Morato, J., Serreli, G., Fito, M., Tyndale, R. F., Deiana, M., & de la Torre, R. (2021). Contribution of biotransformations carried out by the microbiota, drug-metabolizing enzymes, and transport proteins to the biological activities of phytochemicals found in the diet. *Advances in Nutrition, 12*(6), 2172–2189. https://doi.org/10.1093/advances/nmab085

Brasier, A. R. (2010). The nuclear factor-kappaB-interleukin-6 signalling pathway mediating vascular inflammation. *Cardiovascular Research, 86*(2), 211–218. https://doi.org/10.1093/cvr/cvq076

Caminiti, R., Carresi, C., Mollace, R., Macri, R., Scarano, F., Oppedisano, F., … Mollace, V. (2024). The potential effect of natural antioxidants on endothelial dysfunction associated with arterial hypertension. *Frontiers in Cardiovascular Medicine, 11*, 1345218. https://doi.org/10.3389/fcvm.2024.1345218

Cao, H., Chen, X., Jassbi, A. R., & Xiao, J. (2015). Microbial biotransformation of bioactive flavonoids. *Biotechnology Advances, 33*(1), 214–223. https://doi.org/10.1016/j.biotechadv.2014.10.012

Catalan, U., de Las, L., Hazas, M. C., Rubio, L., Fernandez-Castillejo, S., Pedret, A., … Sola, R. (2015). Protective effect of hydroxytyrosol and its predominant plasmatic human metabolites against endothelial dysfunction in human aortic endothelial cells. *Molecular Nutrition & Food Research, 59*(12), 2523–2536. https://doi.org/10.1002/mnfr.201500361

Chang, Y., Chang, T. C., Lee, J. J., Chang, N. C., Huang, Y. K., Choy, C. S., & Jayakumar, T. (2014). Sanguis draconis, a dragon's blood resin, attenuates high glucose-induced oxidative stress and endothelial dysfunction in human umbilical vein endothelial cells. *ScientificWorldJournal, 2014*, Article 423259. https://doi.org/10.1155/2014/423259

Chao, A. C., Lee, T. C., Juo, S. H., & Yang, D. I. (2016). Hyperglycemia increases the production of amyloid Beta-peptide leading to decreased endothelial tight junction. *CNS Neuroscience & Therapeutics, 22*(4), 291–297. https://doi.org/10.1111/cns.12503

Chiou, Y.-S., Wu, J.-C., Huang, Q., Shahidi, F., Wang, Y.-J., Ho, C.-T., & Pan, M.-H. (2014). Metabolic and colonic microbiota transformation may enhance the bioactivities of dietary polyphenols. *Journal of Functional Foods, 7*, 3–25. https://doi.org/10.1016/j.jff.2013.08.006

Cong, X., & Kong, W. (2020). Endothelial tight junctions and their regulatory signaling pathways in vascular homeostasis and disease. *Cellular Signalling, 66*, Article 109485. https://doi.org/10.1016/j.cellsig.2019.109485

Deiana, M., Montoro, P., Jerkovic, I., Atzeri, A., Marijanovic, Z., Serreli, G., … Tuberoso, C. I. G. (2019). First characterization of Pompia intrea candied fruit: The headspace chemical profile, polar extract composition and its biological activities. *Food Research International, 120*, 620–630. https://doi.org/10.1016/j.foodres.2018.11.016

Funk, S. D., Yurdagul, A., Jr., & Orr, A. W. (2012). Hyperglycemia and endothelial dysfunction in atherosclerosis: Lessons from type 1 diabetes. *Int J Vasc Med, 2012*, Article 569654. https://doi.org/10.1155/2012/569654

Galmes, S., Reynes, B., Palou, M., Palou-March, A., & Palou, A. (2021). Absorption, distribution, metabolism, and excretion of the Main olive tree phenols and polyphenols: A literature review. *Journal of Agricultural and Food Chemistry, 69*(18), 5281–5296. https://doi.org/10.1021/acs.jafc.1c00737

Garcia-Villalba, R., Carrasco-Pancorbo, A., Nevedomskaya, E., Mayboroda, O. A., Deelder, A. M., Segura-Carretero, A., & Fernandez-Gutierrez, A. (2010). Exploratory analysis of human urine by LC-ESI-TOF MS after high intake of olive oil: Understanding the metabolism of polyphenols. *Analytical and Bioanalytical Chemistry, 398*(1), 463–475. https://doi.org/10.1007/s00216-010-3899-x

Gloire, G., Legrand-Poels, S., & Piette, J. (2006). NF-kappaB activation by reactive oxygen species: Fifteen years later. *Biochemical Pharmacology, 72*(11), 1493–1505. https://doi.org/10.1016/j.bcp.2006.04.011

Gonzalez, I., Morales, M. A., & Rojas, A. (2020). Polyphenols and AGEs/RAGE axis. *Trends and challenges. Food Res Int, 129*, Article 108843. https://doi.org/10.1016/j.foodres.2019.108843

Gonzalez, P., Lozano, P., Ros, G., & Solano, F. (2023). Hyperglycemia and oxidative stress: An integral, updated and critical overview of their metabolic interconnections. *International Journal of Molecular Sciences, 24*(11). https://doi.org/10.3390/ijms24119352

Gora, I. M., Ciechanowska, A., & Ladyzynski, P. (2021). NLRP3 Inflammasome at the Interface of inflammation, endothelial dysfunction, and type 2 diabetes. *Cells, 10*(2). https://doi.org/10.3390/cells10020314

Hu, Q., Chen, Y., Deng, X., Li, Y., Ma, X., Zeng, J., & Zhao, Y. (2023). Diabetic nephropathy: Focusing on pathological signals, clinical treatment, and dietary regulation. *Biomedicine & Pharmacotherapy, 159*, Article 114252. https://doi.org/10.1016/j.biopha.2023.114252

Jenner, A. M., Rafter, J., & Halliwell, B. (2005). Human fecal water content of phenolics: The extent of colonic exposure to aromatic compounds. *Free Radical Biology & Medicine, 38*(6), 763–772. https://doi.org/10.1016/j.freeradbiomed.2004.11.020

Karkovic Markovic, A., Toric, J., Barbaric, M., & Jakobusic Brala, C. (2019). Hydroxytyrosol, Tyrosol and derivatives and their potential effects on human health. *Molecules, 24*(10). https://doi.org/10.3390/molecules24102001

Kim, M. H., Kim, C. E., & Kim, S. W. (2018). Rosuvastatin inhibits high glucose-stimulated upregulation of VCAM-1 via the MAPK-signalling pathway in endothelial cells. *Acta Cardiologica, 73*(1), 13–18. https://doi.org/10.1080/00015385.2017.1321908

Kim, S. W., Kim, C. E., & Kim, M. H. (2011). Flavonoids inhibit high glucose-induced up-regulation of ICAM-1 via the p38 MAPK pathway in human vein endothelial cells. *Biochemical and Biophysical Research Communications, 415*(4), 602–607. https://doi.org/10.1016/j.bbrc.2011.10.115

Kong, X., Lu, A. L., Yao, X. M., Hua, Q., Li, X. Y., Qin, L., … Su, Q. (2017). Activation of NLRP3 Inflammasome by advanced glycation end products promotes pancreatic islet damage. *Oxidative Medicine and Cellular Longevity, 2017*, 9692546. https://doi.org/10.1155/2017/9692546

Leng, B., Zhang, Y., Liu, X., Zhang, Z., Liu, Y., Wang, H., & Lu, M. (2019). Astragaloside IV suppresses high glucose-induced NLRP3 Inflammasome activation by inhibiting TLR4/NF-kappaB and CaSR. *Mediators of Inflammation, 2019*, 1082497. https://doi.org/10.1155/2019/1082497

Li, B., Li, Y., Liu, K., Wang, X., Qi, J., Wang, B., & Wang, Y. (2017). High glucose decreases claudins-5 and -11 in cardiac microvascular endothelial cells: Antagonistic effects of tongxinluo. *Endocrine Research, 42*(1), 15–21. https://doi.org/10.3109/07435800.2016.1163723

Lin, F., Yang, Y., Wei, S., Huang, X., Peng, Z., Ke, X., … Song, Y. (2020). Hydrogen sulfide protects against high glucose-induced human umbilical vein endothelial cell injury through activating PI3K/Akt/eNOS pathway. *Drug Design, Development and Therapy, 14*, 621–633. https://doi.org/10.2147/DDDT.S242521

Liu, C., Chu, D., Kalantar-Zadeh, K., George, J., Young, H. A., & Liu, G. (2021). Cytokines: From clinical significance to quantification. *Adv Sci (Weinh), 8*(15), Article e2004433. https://doi.org/10.1002/advs.202004433

Manach, C., Scalbert, A., Morand, C., Remesy, C., & Jimenez, L. (2004). Polyphenols: Food sources and bioavailability. *The American Journal of Clinical Nutrition, 79*(5), 727–747. https://doi.org/10.1093/ajcn/79.5.727

Pandey, K. B., & Rizvi, S. I. (2009). Plant polyphenols as dietary antioxidants in human health and disease. *Oxidative Medicine and Cellular Longevity, 2*(5), 270–278. https://doi.org/10.4161/oxim.2.5.9498

Pastor, A., Rodriguez-Morato, J., Olesti, E., Pujadas, M., Perez-Mana, C., Khymenets, O., … de la Torre, R. (2016). Analysis of free hydroxytyrosol in human plasma following the administration of olive oil. *Journal of Chromatography. A, 1437*, 183–190. https://doi.org/10.1016/j.chroma.2016.02.016

Pavillard, L. E., Marin-Aguilar, F., Bullon, P., & Cordero, M. D. (2018). Cardiovascular diseases, NLRP3 inflammasome, and western dietary patterns. *Pharmacological Research, 131*, 44–50. https://doi.org/10.1016/j.phrs.2018.03.018

Plotnikov, A., Zehorai, E., Procaccia, S., & Seger, R. (2011). The MAPK cascades: Signaling components, nuclear roles and mechanisms of nuclear translocation. *Biochimica et Biophysica Acta, 1813*(9), 1619–1633. https://doi.org/10.1016/j.bbamcr.2010.12.012

Popov, D. (2010). Endothelial cell dysfunction in hyperglycemia: Phenotypic change, intracellular signaling modification, ultrastructural alteration, and potential clinical outcomes. *International Journal of Diabetes Mellitus, 2*(3), 189–195. https://doi.org/10.1016/j.ijdm.2010.09.002

Qian, Y., Ducatman, A., Ward, R., Leonard, S., Bukowski, V., Lan Guo, N., … Castranova, V. (2010). Perfluorooctane sulfonate (PFOS) induces reactive oxygen species (ROS) production in human microvascular endothelial cells: Role in endothelial permeability. *Journal of Toxicology and Environmental Health. Part A, 73*(12), 819–836. https://doi.org/10.1080/15287391003689317

Rajendran, P., Rengarajan, T., Thangavel, J., Nishigaki, Y., Sakthisekaran, D., Sethi, G., & Nishigaki, I. (2013). The vascular endothelium and human diseases. *International Journal of Biological Sciences, 9*(10), 1057–1069. https://doi.org/10.7150/ijbs.7502

Rezabakhsh, A., Nabat, E., Yousefi, M., Montazersaheb, S., Cheraghi, O., Mehdizadeh, A., … Garjani, A. (2017). Endothelial cells' biophysical, biochemical, and chromosomal aberrancies in high-glucose condition within the diabetic range. *Cell Biochemistry and Function, 35*(2), 83–97. https://doi.org/10.1002/cbf.3251

Robles-Osorio, M. L., & Sabath, E. (2023). Tight junction disruption and the pathogenesis of the chronic complications of diabetes mellitus: A narrative review. *World Journal of Diabetes, 14*(7), 1013–1026. https://doi.org/10.4239/wjd.v14.i7.1013

Rubió, L., Farràs, M., de La Torre, R., Macià, A., Romero, M.-P., Valls, R. M., … Motilva, M.-J. (2014). Metabolite profiling of olive oil and thyme phenols after a sustained intake of two phenol-enriched olive oils by humans: Identification of compliance markers. *Food Research International, 65*, 59–68. https://doi.org/10.1016/j.foodres.2014.05.009

Rubio, L., Valls, R. M., Macia, A., Pedret, A., Giralt, M., Romero, M. P., … Motilva, M. J. (2012). Impact of olive oil phenolic concentration on human plasmatic phenolic metabolites. *Food Chemistry, 135*(4), 2922–2929. https://doi.org/10.1016/j.foodchem.2012.07.085

Schroder, K., & Tschopp, J. (2010). The inflammasomes. *Cell, 140*(6), 821–832. https://doi.org/10.1016/j.cell.2010.01.040

Serreli, G., & Deiana, M. (2018). Biological relevance of extra virgin olive oil polyphenols metabolites. *Antioxidants (Basel), 7*(12). https://doi.org/10.3390/antiox7120170

Serreli, G., & Deiana, M. (2019). In vivo formed metabolites of polyphenols and their biological efficacy. *Food & Function, 10*(11), 6999–7021. https://doi.org/10.1039/c9fo01733j

Serreli, G., & Deiana, M. (2020). Extra virgin olive oil polyphenols: Modulation of cellular pathways related to oxidant species and inflammation in aging. *Cells, 9*(2), 478. https://doi.org/10.3390/cells9020478

Serreli, G., Le Sayec, M., Diotallevi, C., Teissier, A., Deiana, M., & Corona, G. (2021). Conjugated metabolites of Hydroxytyrosol and Tyrosol contribute to the maintenance of nitric oxide balance in human aortic endothelial cells at physiologically relevant concentrations. *Molecules, 26*(24). https://doi.org/10.3390/molecules26247480

Serreli, G., Le Sayec, M., Thou, E., Lacour, C., Diotallevi, C., Dhunna, M. A., … Corona, G. (2021). Ferulic acid derivatives and Avenanthramides modulate endothelial function through maintenance of nitric oxide balance in HUVEC cells. *Nutrients, 13*(6). https://doi.org/10.3390/nu13062026

Serreli, G., Melis, M. P., Corona, G., & Deiana, M. (2019). Modulation of LPS-induced nitric oxide production in intestinal cells by hydroxytyrosol and tyrosol metabolites: Insight into the mechanism of action. *Food and Chemical Toxicology, 125*, 520–527. https://doi.org/10.1016/j.fct.2019.01.039

Sun, T., Chen, Q., Zhu, S. Y., Wu, Q., Liao, C. R., Wang, Z., … Chen, J. T. (2019). Hydroxytyrosol promotes autophagy by regulating SIRT1 against advanced oxidation protein product-induced NADPH oxidase and inflammatory response. *International Journal of Molecular Medicine, 44*(4), 1531–1540. https://doi.org/10.3892/ijmm.2019.4300

Vijakumaran, U., Shanmugam, J., Heng, J. W., Azman, S. S., Yazid, M. D., Haizum Abdullah, N. A., & Sulaiman, N. (2023). Effects of Hydroxytyrosol in endothelial functioning: A comprehensive review. *Molecules, 28*(4). https://doi.org/10.3390/molecules28041861

Volpe, C. M. O., Villar-Delfino, P. H., Dos Anjos, P. M. F., & Nogueira-Machado, J. A. (2018). Cellular death, reactive oxygen species (ROS) and diabetic complications. *Cell Death & Disease, 9*(2), 119. https://doi.org/10.1038/s41419-017-0135-z

Wan, Z., Fan, Y., Liu, X., Xue, J., Han, Z., Zhu, C., & Wang, X. (2019). NLRP3 inflammasome promotes diabetes-induced endothelial inflammation and atherosclerosis. *Diabetes Metab Syndr Obes, 12*, 1931–1942. https://doi.org/10.2147/DMSO.S222053

Yamagishi, S. (2011). Role of advanced glycation end products (AGEs) and receptor for AGEs (RAGE) in vascular damage in diabetes. *Experimental Gerontology, 46*(4), 217–224. https://doi.org/10.1016/j.exger.2010.11.007

Yuan, T., Yang, T., Chen, H., Fu, D., Hu, Y., Wang, J., … Xie, X. (2019). New insights into oxidative stress and inflammation during diabetes mellitus-accelerated atherosclerosis. *Redox Biology, 20*, 247–260. https://doi.org/10.1016/j.redox.2018.09.025

Zeka, K., Ruparelia, K., Arroo, R. R. J., Budriesi, R., & Micucci, M. (2017). Flavonoids and their metabolites: Prevention in cardiovascular diseases and diabetes. *Diseases, 5*(3). https://doi.org/10.3390/diseases5030019

Zhang, C. (2008). The role of inflammatory cytokines in endothelial dysfunction. *Basic Research in Cardiology, 103*(5), 398–406. https://doi.org/10.1007/s00395-008-0733-0

Zhang, X., Wang, T., Gui, P., Yao, C., Sun, W., Wang, L., … Wu, Q. (2013). Resolvin D1 reverts lipopolysaccharide-induced TJ proteins disruption and the increase of cellular permeability by regulating IkappaBalpha signaling in human vascular endothelial cells. *Oxidative Medicine and Cellular Longevity, 2013*, Article 185715. https://doi.org/10.1155/2013/185715

Zodio, S., Serreli, G., Melis, M. P., Franchi, B., Boronat, A., de la Torre, R., & Deiana, M. (2024). Protective effect of hydroxytyrosol and tyrosol metabolites in LPS-induced vascular barrier derangement in vitro. *Frontiers in Nutrition, 11*, 1350378. https://doi.org/10.3389/fnut.2024.1350378